CROATICA CHEMICA ACTA CCACAA **72** (2–3) 645–661 (1999)

ISSN-0011-1643
CCA-2603

Original Scientific Paper

A Study of the Mn, Co and Ni Environment in the As-synthesized and Rehydrated-calcined Aluminophosphate with Chabazite-like Topology*

Nevenka Rajić,[a] *Iztok Arčon,*[b,c] *Venčeslav Kaučič,*[a,**] *and Alojz Kodre*[c,d]

[a] *National Institute of Chemistry, Hajdrihova 19, 1000 Ljubljana, Slovenia*

[b] *School of Environmental Sciences, 5001 Nova Gorica, Slovenia*

[c] *Institute Jožef Stefan, 1000 Ljubljana, Slovenia*

[d] *Department of Physics, Faculty of Mathematics and Physics, University of Ljubljana, 1000 Ljubljana, Slovenia*

Received September 18, 1998; revised April 21, 1999; accepted April 23, 1999

Diffuse-reflectance spectroscopy (DRS), X-ray absorption near-edge structure (XANES) and extended X-ray absorption fine structure (EXAFS) methods are applied to an investigation of Mn, Co and Ni local environments in MnAlPO, CoAlPO, and NiAlPO materials with chabazite-like topology. For all three products, insertion of the transition metals into tetrahedral Al-sites has been found. Calcination and rehydration of the as-synthesised materials cause a change of the oxidation number and co-ordination geometry of Mn and Co, while the oxidation and co-ordination number of Ni remain unaffected.

Key words: aluminophosphates; molecular sieves; MAPO-34; chabazite-like; EXAFS, XANES; diffuse reflectance spectroscopy.

---

* Dedicated to Professor Boris Kamenar on the occasion of his 70th birthday.

** Author to whom correspondence should be addressed. (E-mail: kaucic@ki.si.)

INTRODUCTION

Aluminophosphate-based molecular sieves (AlPO) have attracted great attention during the last few years. The considerable interest can be explained by their enhanced structural diversity as well as by the possibility of insertion of more than fifteen elements by isomorphous substitution of phosphorous or/and aluminium into the porous AlPO's framework.[1]

Transition metal modified AlPOs (MAPO) are of particular interest since they encompass two important phenomena: catalytic activity of the transition metal modified solids and the shape selectivity of the zeolitic host. In this context, the oxidation state, location and dispersion of the transition metal ions are crucial for understanding the catalytic properties of these materials.

Various techniques have been used to study the nature of transition metal insertion. Visible spectroscopy, ESR, FTIR and NMR have been widely applied.[2–11] Single crystal X-ray diffraction method certainly offers even more valuable information; however, problems in growing suitable single crystals impose limitations on the use of this method. XANES and EXAFS have successfully been applied so far to characterise the local co-ordination of Co(II), Mn(II) and Ni(II) ions in polycrystalline zeolite A and Y[12–15] as well as to investigate the structure of acid sites in some CoAlPO molecular sieves. [16,17]

In this paper, we have used the DRS, XANES and EXAFS methods for the investigation of the location of manganese(II), cobalt(II), and nickel(II) cations inserted into a chabazite-like AlPO framework. The AlPO-matrix was prepared using a fluoride synthetic route. This procedure yields a triclinic precursor of chabazite-like framework in which fluoride bridges increase the co-ordination number of some of the aluminium atoms from 4 to 6, causing a triclinic deformation of the rhombohedral chabazite structure.[18] Consequently, the transition metal cations have theoretically two possibilities of insertion into the AlPO's framework: the sites of the tetrahedral aluminium as well as octahedral ones. This appears specially interesting for Ni(II) insertion since, according to the ligand-field stabilisation energy (LFSE) data, Ni(II) shows the lowest preference towards tetrahedral coordination relative to the octahedral one in comparison with Mn(II) and Co(II).[19] Upon calcination, the fluoride bridges in the triclinically deformed chabazite-like AlPO framework are destroyed and the calcined product possesses a regular chabazite-like topology (in which a strict alternation of the tetrahedral AlO_4 and PO_4 units is present).[20] Thus, DRS, EXAFS and XANES studies have also provided additional information about the local structural changes around the transition metal ions resulting from calcination and rehydration of the as-synthesised materials.

Moreover, it has been known that zeolitic framework can stabilise some co-ordination geometries that are not common for the transition metal ions.[21] Since an aluminophosphate framework has also been visualised as a polidentate ligand, the results obtained by DRS have a practical importance: they give useful information about the electronic spectra of transition metal complexes with uncommon co-ordination geometries.

EXPERIMENTAL

MAPO materials were synthesised hydrothermally in a HF medium according to the previously published procedure.[20] White, royal blue, and pale blue products were obtained for MnAlPO, CoAlPO and NiAlPO materials, respectively. X-ray diffraction analysis and electron scanning microscopy revealed a high crystallinity and phase purity of each of the as-synthesised materials. Energy-dispersive X-ray emission analysis performed on the high quality single crystals of the as-synthesised products gave the following product formula, calculated on anhydrous basis: MnAlPO: $(Mn_{0.05}Al_{0.96}PO_4)_6 \cdot (C_5H_7N)_2 \cdot F_2$; CoAlPO: $(Co_{0.05}Al_{0.95}PO_4)_6 \cdot (C_5H_7N)_2 \cdot F_2$; NiAlPO: $(Ni_{0.04}Al_{0.95}PO_4)_6 \cdot (C_5H_7N)_2 \cdot F_2$. The sum Al + M = P for the products lies within the experimental error range, indicating that all transition metal cations have substituted aluminium in the framework.

The samples were calcined in air at 800 °C for 2 h and stored under controlled humid atmosphere prior to the XANES, EXAFS and DRS measurements. These samples are referred to as the rehydrated-calcined samples in further discussion.

DRS were obtained on a Varian MS 80 UV/VIS spectrophotometer in the 900–300 nm range, with MgO as a standard.

EXAFS spectra at Mn, Co, and Ni K-edge were measured at the EXAFS II station in HASYLAB at DESY (Hamburg, Germany). Synchrotron radiation from DORIS storage was focused by an Au-coated mirror on a Si(111) double-crystal monochromator with 1.5 eV resolution at 7 keV. Harmonics were effectively eliminated by detuning the monochromator crystal using a stabilisation feedback control. Powdered samples were prepared on multiple layers of adhesive tape with a total absorption thickness of $\mu d \approx 2$ above the K-edge of the investigated element. Reference spectra on the empty tapes were taken under identical conditions. Standard stepping progression within 1000 eV region above the edge was adopted. Exact energy calibration was established with simultaneous absorption measurements on appropriate metal foil.

RESULTS AND DISCUSSION

The XRD patterns of all as-synthesised products showed the materials to be crystallographically pure triclinic chabazite-like aluminophosphate. The triclinic deformation was removed by calcination, yielding the rhombohedral chabazite-like MAPO framework. All calcined products show a particular sensitivity towards hydration, resulting in a novel triclinic deforma-

tion of the chabazite-like MAPO's lattice.[1] The phenomenon is quite reversible: thermal evacuation of the rehydrated samples causes a complete return to the regular chabazite-like material. The corresponding patterns have been reported elsewhere.[20]

The first insight into the co-ordination geometry of inserted transition metals is obtained by DRS. Figure 1 shows DR spectra of the as-synthesised and the rehydrated-calcined MnAlPO products. It is evident that the spec-

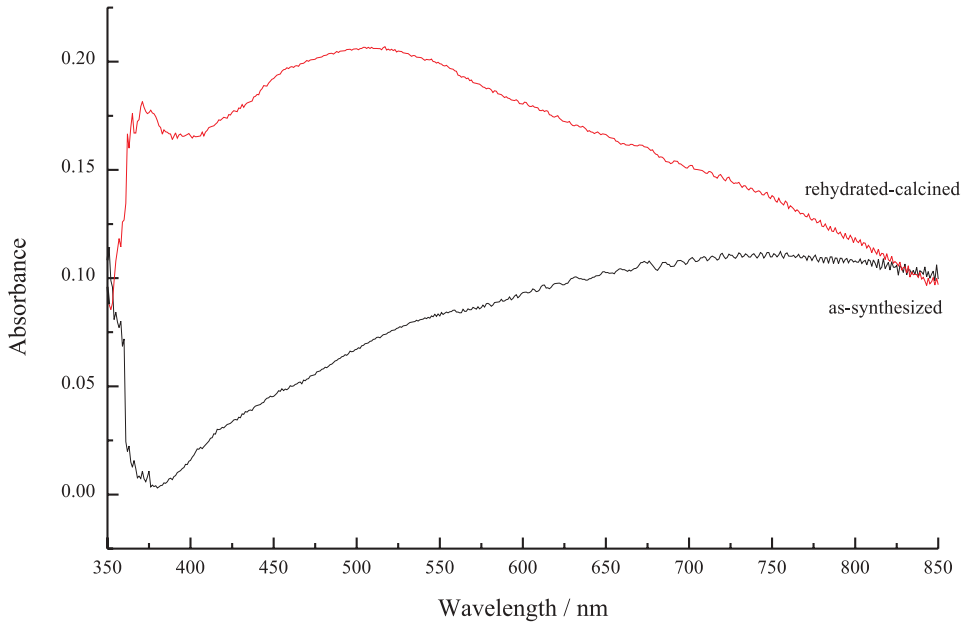

Figure 1. DR spectra of MnAlPO products.

trum of the as-synthesised material is not very informative, unlike that of the rehydrated-calcined sample in which a strong absorption maximum at ≈ 500 nm appears. The white as-synthesised MnAlPO product shows several colour changes during calcination and rehydration: becoming green upon calcination, blue upon cooling, and finally pink-grey upon hydration. The green-blue colour change could presumably be attributed to a thermochromic effect. Namely, it is known that manganese(II)-doped zinc silicate is a useful phosphor giving a green colour emission.[22] The final colour change, however, could be attributed to the oxidation of Mn(II) to Mn(III). Namely, the position of the absorption maximum in the spectrum of the rehydrated-calcined MnAlPO is similar to that of Mn(III) complexes octahedrally co-

ordinated by oxygen-donor ligands.[23] This has two consequences: 1) oxidation of Mn(II) to Mn(III) occurs upon calcination, and 2) since LFSE data show that the Mn(III) is more stable in an octahedral environment than in the tetrahedral one,[19] it is rather predictable that upon hydration the tetrahedral framework Mn(III) species should readily increase the co-ordination number from 4 to 6.

DR spectrum of the as-synthesised CoAlPO product (Figure 2) entirely corresponds to tetrahedrally co-ordinated Co(II) species inserted in an

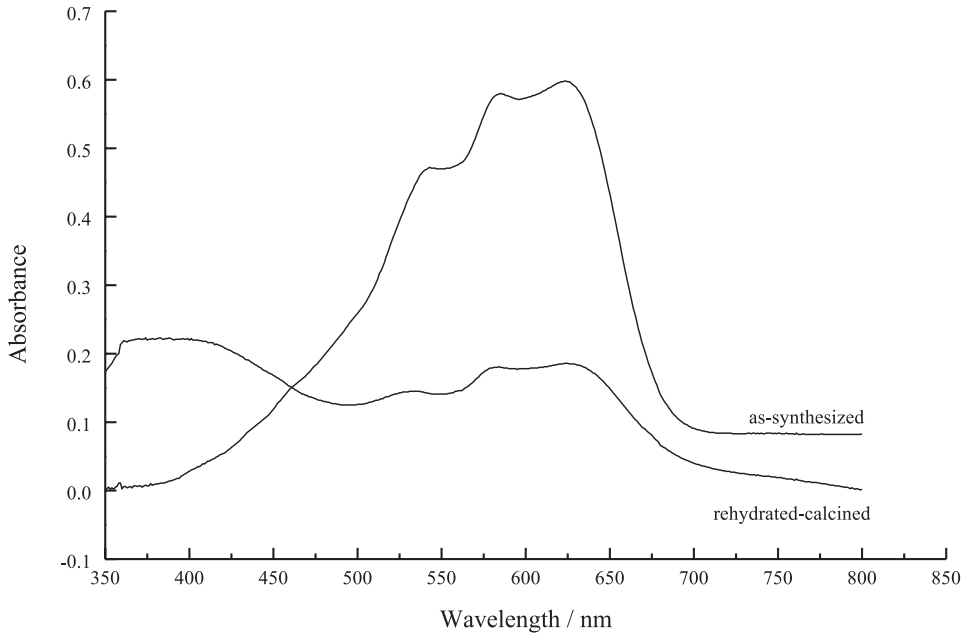

Figure 2. DR spectra of CoAlPO products.

AlPO-matrix.[4] Upon calcination and ensuing rehydration, the CoAlPO material also shows a colour change as follows: 1) from blue to yellow, immediately after calcination, and 2) from yellow to green after exposure of the calcined product to humid atmosphere. The rehydrated-calcined product shows a strong broad absorption at about 370 nm and three weak absorptions at wavelengths that completely correspond to the maxima in the spectrum of the as-synthesised CoAlPO material. The strong broad absorption can be attributed to tetrahedral Co(III) [4] while the weak absorptions are most probably due to the tetrahedral Co(II). Namely, it has recently been shown that the framework Co(II) is readily oxidised to the Co(III) upon calcination in

an O_2 atmosphere.[4,20] However, in our case, the appearance of the absorption maxima corresponding to the divalent tetrahedral cobalt indicates that a part of the oxidised trivalent cobalt species is reduced to Co(II) upon exposure of the calcined product to the humid atmosphere. In this manner, the green colour of the rehydrated-calcined product can be accounted for (*i.e.* yellow + blue).

The DR spectra of NiAlPO samples are given in Figure 3. The material shows only one colour change: from pale blue to yellow. The exposure of the calcined sample to the humid atmosphere has no influence on its yellow col-

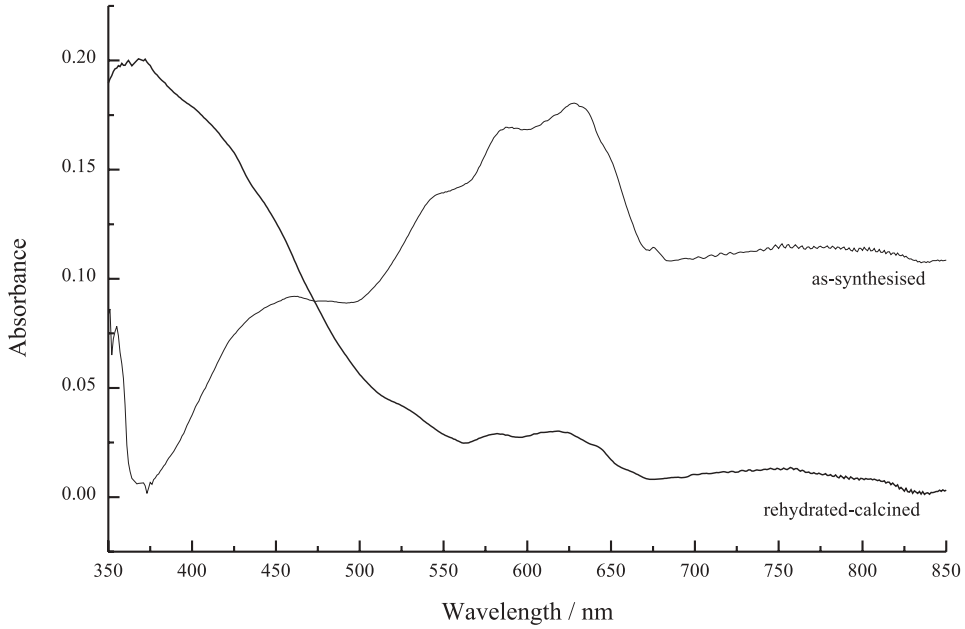

Figure 3. DR spectra of NiAlPO products.

our. Furthermore, the spectra of the as-synthesised and the calcined samples differ from each other. Positions of the absorption maxima in both NiAlPO samples are in general similar to those that have been reported for Ni(II) ions in a distorted tetrahedral symmetry,[5] confirming the framework position of Ni(II) (it should be kept in mind that the unit cell formula indicates that Ni(II) ions replace the framework aluminium species). However, the spectrum of the rehydrated-calcined form of this material is somewhat different from the as-synthesised one. While the most intensive maxima in

the spectrum of the as-synthesised sample (at 580 and 620 nm) have greatly diminished intensities in the spectrum of the calcined form, a new intensive maximum at 370 nm appears in the spectrum of the rehydrated-calcined product (wich might be responsible for the change of colour). It might be expected, by analogy to MnAlPO and CoAlPO, that the colour change could be due to the oxidation of Ni(II) to Ni(III). However, Ni^{3+} is very rare.[24] Accordingly, the colour change (and the changes in the DR spectrum) could only be attributed to an additional deformation of the tetrahedral Ni(II) geometry. This is supported by the fact that some pseudo-tetrahedral Ni(II) complexes show an intense charge-transfer band at ≈ 400 nm.[25]

The Mn, Co and Ni K-edge XANES are used to identify the local symmetry and the average oxidation number of transition metal atoms. The shape of the edge and the pre-edge region resonances can be used as a fingerprint for identification of the local symmetry of the inserted metals. A single pre-edge peak is characteristic of the atoms located at the sites without a centre of inversion. For transition metal atoms located at the octahedrally co-ordinated sites (having the centre of inversion), two small resonances are found in the pre-edge region.[26–28] Furthermore, the energy position of the edge is correlated with the oxidation number of the investigated atom in the sample: an increase of the oxidation state causes a shift of the absorption edge towards higher energies. [28,29]

The normalised Mn XANES spectra of the MnAlPO samples as well as the spectra of the reference samples with well known oxidation numbers (such as $Mn^{II}O$, $K_3[Mn^{III}(C_2O_4)_3] \cdot 3H_2O$, $Mn^{IV}O_2$, and Mn^0 metal) are shown in Figure 4. The K-shell contribution is obtained by removing the extrapolated pre-edge (–200 ... –50 eV) trend. The spectra are normalised to a unit edge jump. The zero energy is taken at the first inflection point in the Mn metal spectrum at 6539.0 eV, which marks the 1s ionisation threshold in Mn metal.

A single pre-edge peak is seen in the XANES spectra of both MnAlPO samples, indicating the presence of Mn atoms at sites without the centre of inversion. The intensity of the peaks is, however, much lower than in systems where the Mn atom is tetrahedrally co-ordinated by four oxygen atoms forming regular MnO_4 species.[29] This indicates that the co-ordination geometry of Mn atoms in both MnAlPO samples is distorted (*vide infra*). Moreover, a shift of the Mn K-edge towards higher energies is found after calcination, reflecting a partial oxidation of Mn in the rehydrated-calcined sample. This agrees with the DR data, which indicate the oxidation of Mn(II) to Mn(III) upon calcination.

The K-edge energy shifts for both MnAlPO products and reference samples are given in Table I. The energy position of the edge is taken at the edge inflection point denoted by the arrow in Figure 4, determined as the

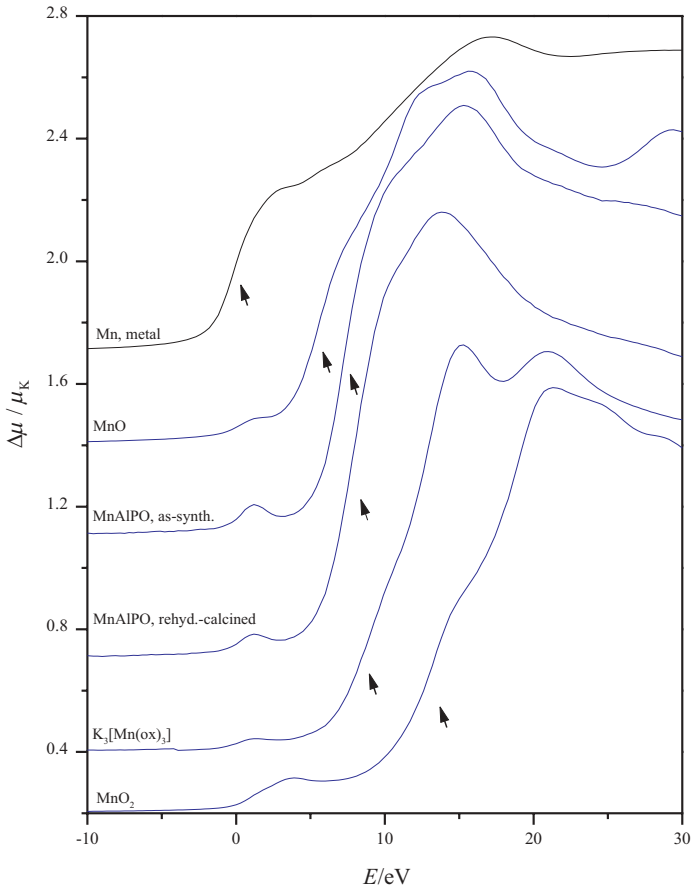

Figure 4. Normalised Mn K-edge profiles, displaced vertically, for the MnAlPO and reference samples. Arrows denote the position of the Mn K-edge. Energy scale is relative to the Mn K-edge of metal (6539.0 eV).

TABLE I

The energy shift ΔE_K of the Mn K-edge and an average Mn oxidation number in the MnAlPO and reference samples

Sample	ΔE_K/eV	Mn oxidation number
MnAlPO, as-synthesized	7.5(2)	+ 2.5(3)
MnAlPO, rehydrated-calcined	8.4(2)	+ 2.7(3)
MnO	5.7(2)	+ 2
$K_3[Mn(C_2O_4)_3] \cdot 3H_2O$	9.3(2)	+ 3
MnO_2	13.5(2)	+ 4

Numbers in parentheses correspond to the standard error in the last significant digit.

tip of the peak in the derivative spectrum. The reference samples have been used to deduce the interdependence of the Mn K-edge shift and the oxidation number.

The data strongly support the empirically established linear interdependence of the edge shift and valence [28] (as shown in Figure 5). Using the best fit to the reference data, the average Mn oxidation number in the MnAlPO samples is calculated to be 2.5 for the as-synthesised and 2.7 for the

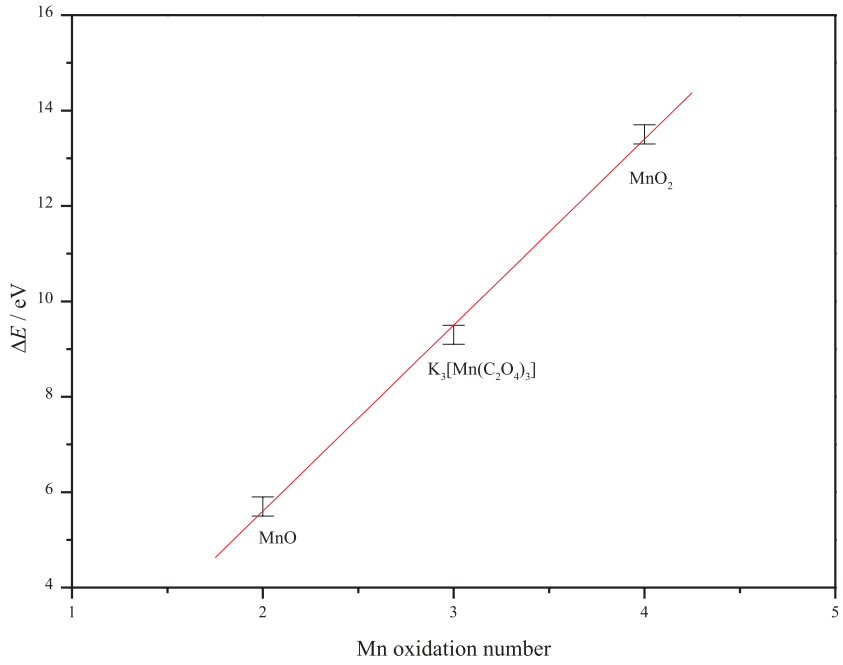

Figure 5. Energy positions of the Mn K-edge of the reference samples *vs.* Mn oxidation numbers. The best linear fit is shown by a solid line.

rehydrated-calcined MnAlPO. The average Mn oxidation number of 2.5 obtained for the as-synthesised MnAlPO is however unexpected. It should indicate that, upon crystallisation of MnAlPO, a part of Mn(II) is oxidised to Mn(III). At this moment, no rational explanation for this can be given since the oxidation of Mn(II) to Mn(III) in an acidic medium (as in the present reaction) is not favourable.[30]

The normalised Co K-edge XANES spectra of the CoAlPO samples are shown in Figure 6. The characteristic pre-edge peak of the tetrahedrally coordinated cobalt species [17] can be seen in both the as-synthesised and the

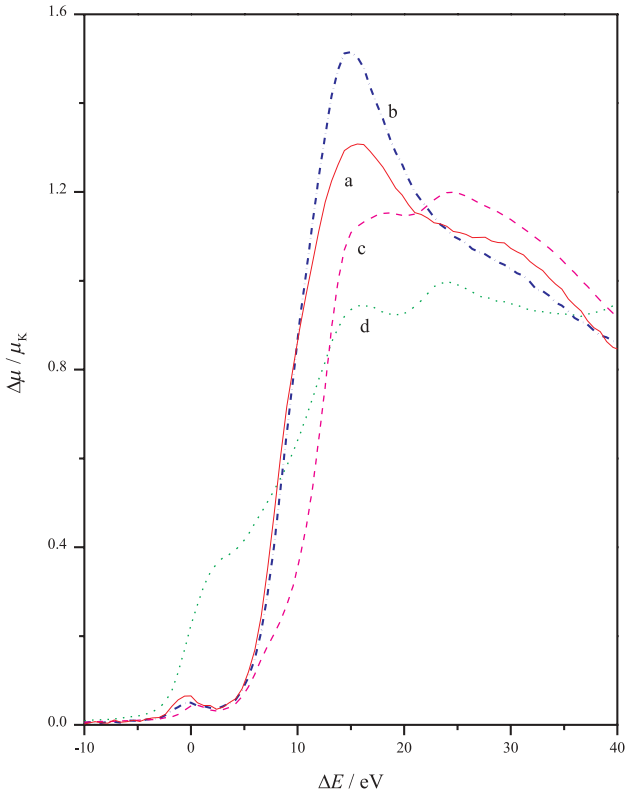

Figure 6. Normalised Co K-edge profiles of CoAlPO, as-synthesised (a); CoAlPO, rehydrated-calcined (b); $[Co(C_2H_8N_2)_3]Cl_3 \cdot 4H_2O$ (c); Co, metal (d).

rehydrated-calcined samples. The presence of Co(II) in the as-synthesised sample can be deduced from the Co K-edge energy shift (Tabe II). In the rehydrated-calcined sample, there is a slight shift of the edge to higher en-

TABLE II

The energy shift ΔE_K of the Co K-edge and an average Co oxidation number in the CoAlPO and reference samples

Sample	ΔE_K/eV	Co oxidation number
CoAlPO, as-synthesized	8.4(2)	+ 1.9(1)
CoAlPO, rehydrated-calcined	9.0(2)	+ 2.1(1)
$[Co(C_2H_8N_2)_3]Cl_3 \cdot 4H_2O$	13.2(2)	+ 3
Co, metal	0.0(1)	0

Numbers in parentheses correspond to the standard error in the last significant digit.

ergy, indicating a partial oxidation of Co(II) to Co(III) upon calcination (confirming the finding of the DR measurements).

The Ni K-edge XANES spectra of the NiAlPO samples are shown in Figure 7. It is seen that both samples show identical Ni K-edge profiles, indicating that calcination of the NiAlPO does not influence the Ni(II) oxidation state. Furthermore, the characteristic pre-edge peak suggests a tetrahedral co-ordination of Ni(II) species.

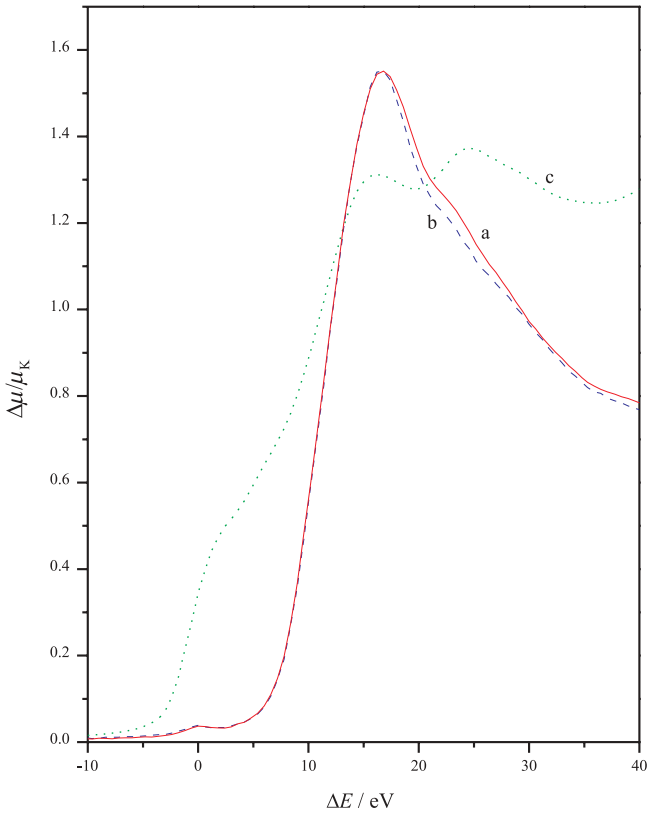

Figure 7. Normalised Ni K-edge profiles of NiAlPO, as-synthesised (a); NiAlPO, rehydrated-calcined (b); Ni, metal (c).

EXAFS spectra measured on the as-synthesised and the rehydrated-calcined MnAlPO, CoAlPO, and NiAlPO samples (Figure 8) have been analysed by the University of Washington analysis programs using FEFF6 code for *ab-initio* calculation of scattering paths.[31,32] Only the contributions from the closest shells of neighbours in the R range of 1.2 to 2.1 Å are fitted.

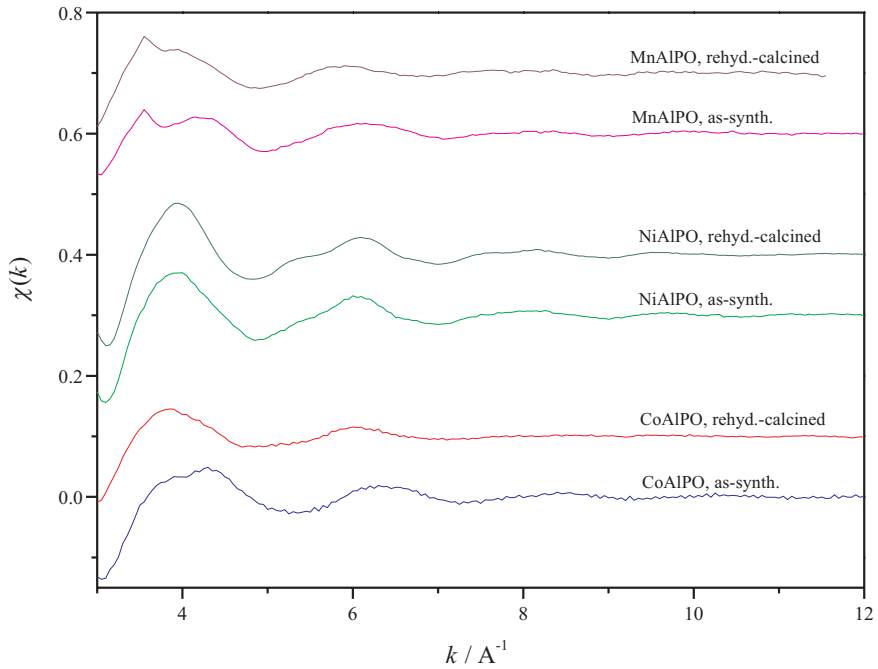

Figure 8. Standard EXAFS spectra of MnAlPO, CoAlPO, and NiAlPO products.

Fourier transforms and Fourier filtered first shell contribution of k^3 weighted $\chi(k)$ spectra are shown in Figure 9.

Four oxygen atoms are identified in the first co-ordination shell around the transition metal atoms in all the three as-synthesised samples. This confirms insertion of the transition metal cations into the AlPO framework. After calcination and rehydration, changes in the local environment of the transition metal atoms are observed for MnAlPO and CoAlPO, but not for NiAlPO samples. A complete list of best fit parameters is given in Table III.

For the rehydrated-calcined MnAlPO, six oxygen atoms are found in the local environment of Mn. There are four oxygens at 2.10 Å and two at a larger distance of 2.37 Å, indicating a distorted octahedral geometry around Mn species. Since the distortion of the octahedral geometry of Mn(III) is quite predictable (most octahedral d^4 complexes exhibit the Jahn-Teller effect), this could be an additional support that the Mn(II) is oxidised to

Figure 9. Fourier transforms and Fourier filtered first shell contribution of k^3 weighted $\chi(k)$ spectra of as-synthesized and the rehydrated-calcined MnAlPO, and NiAlPO samples: experiment (solid line); fit (dotted line). ⇒

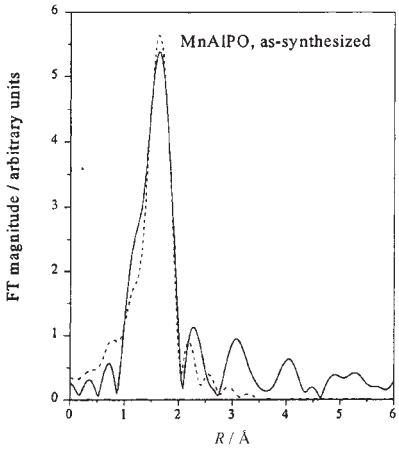
MnAlPO, as-synthesized
FT magnitude / arbitrary units
R / Å

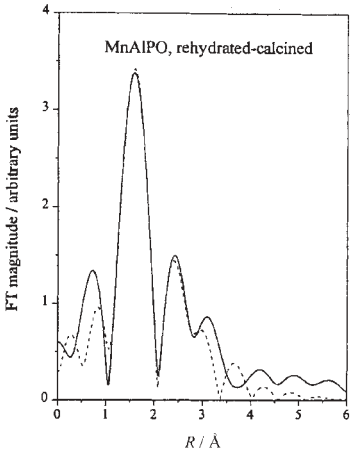
MnAlPO, rehydrated-calcined
FT magnitude / arbitrary units
R / Å

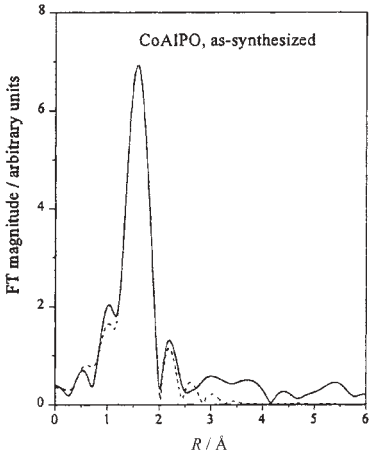
CoAlPO, as-synthesized
FT magnitude / arbitrary units
R / Å

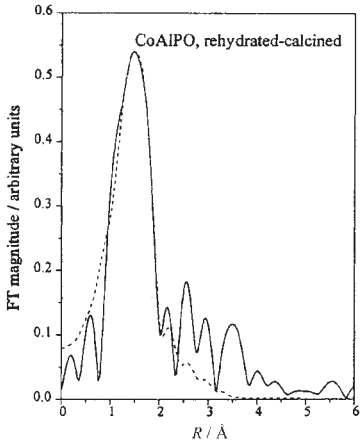
CoAlPO, rehydrated-calcined
FT magnitude / arbitrary units
R / Å

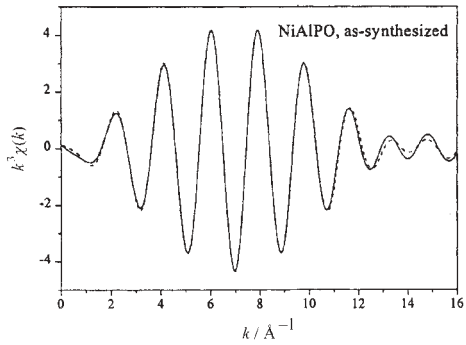
NiAlPO, as-synthesized
k³χ(k)
k / Å⁻¹

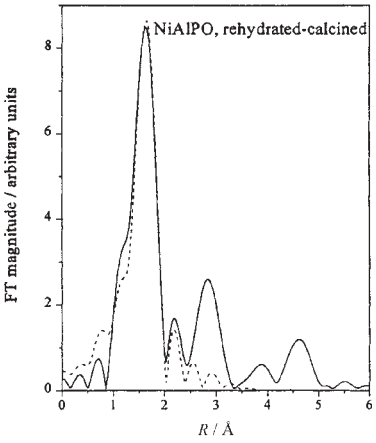
NiAlPO, rehydrated-calcined
FT magnitude / arbitrary units
R / Å

TABLE III

Parameters of the first coordination sphere of metal atoms in the MAlPO samples: N – coordination number, R – metal–oxygen distance, and σ^2 – Debye-Waller factor

Sample	As-synthesized			Rehydrated-calcined		
	N	R/Å	σ^2/Å^2	N	R/Å	σ^2/Å^2
MnAlPO	4.0(4)	2.02(2)	0.005(1)	4.0(4)	2.10(2)	0.005(1)
	/	/	/	2.0(4)	2.37(2)	0.003(1)
CoAlPO	3.9(3)	1.96(1)	0.0032(6)	1.6(2)	1.90(2)	0.003(1)
	/	/	/	2.3(2)	2.06(2)	0.003(1)
NiAlPO	4.0(5)	2.05(1)	0.0044(8)	3.9(5)	2.05(1)	0.005(1)

Numbers in parentheses correspond to the standard error in the last significant digit.

Mn(III) upon calcination. It could be added that the average Mn–O distance of 2.19 Å is in reasonable agreement with the Mn–O distance of 2.09 Å reported for MnAPO-34. [33]

For the rehydrated-calcined CoAlPO sample, four oxygens are found in the Co local environment (as in the as-synthesised sample). This shows that cobalt does not increase its co-ordination number upon hydration of the calcined CoAlPO. However, the cobalt environment is split into two close subsets: the best fit is obtained with 1.6 oxygens at the distance of 1.90 Å and 2.3 oxygens at 2.06 Å. This also indicates that the tetrahedral Co co-ordination geometry is deformed. The result is consistent with the electron spin resonance data found for the calcined CoAlPO-5.[34] Moreover, the average Co–O distance (1.94 Å) agrees well with the reported Co–O distance of 1.96 Å of CoAPO-H3. [35]

The local structure around Ni in the rehydrated-calcined NiAlPO sample shows a single shell of four oxygens. The same Ni–O distance of 2.05 Å (the latter agrees well with the reported Ni–O distance of 2.02 Å for the dehydrated Ni–Y)[15] is obtained for both the as-synthesised and the rehydrated-calcined NiAlPO. This indicates that the calcination (and rehydration) not only does not influence oxidation and the co-ordination number of Ni(II) but also does not affect Ni(II) co-ordination geometry. However, an increase of the peak at about 3 Å observed in the Fourier transform EXAFS spectrum of the rehydrated-calcined NiAlPO relative to as-synthesised sample indicates that a change in the second co-ordination shell of Ni(II) occurs upon calcination (Figure 9). This is in agreement with DRS measurements, which indicate that a deformation of Ni(II) co-ordination geometry occurs upon calcination.

CONCLUSIONS

Insertion of Mn, Co and Ni in the aluminophosphate lattice with chabazite-like topology has been investigated using DRS, XANES, and EXAFS studies. In the as-synthesised materials, all methods reveal the tetrahedral co-ordination around the transition metal cations, confirming that they are constituents of the chabazite-like framework (replacing the framework Al atoms). However, the calcination and rehydration of the as-synthesised materials cause changes in the local environment of the transition metal cations. Upon calcination, Mn(II) and Co(II) are oxidised to Mn(III) and Co(III). Moreover, rehydration causes an increase of the co-ordination number of Mn(III), while Co(III) is reduced to the divalent state. The reduced cobalt species exhibit a deformed tetrahedral co-ordination geometry.

In contrast, NiAlPO remains almost unchanged upon calcination and rehydration. Not only that the oxidation number of Ni does not change upon calcination, but hydration does not affect the co-ordination number of Ni(II) either. This relative stability of Ni(II) in comparison to Mn(II) and Co(II) could be explained by considering ionisation energies of these metals. While the third ionisation energy of Co and Mn exhibits a similar value, the third ionisation energy of Ni is higher by about 160 kJ/mol.[36]

However, the DRS and EXAFS measurements on the NiAlPO samples indicate that some changes still occur upon calcination of NiAlPO. This can be attributed to the changes in the second co-ordination sphere of Ni(II). The explanation could be as follows. The removal of triclinic deformation in the AlPO framework (which occurs upon calcination by destruction of the fluoride bridges) causes a framework perturbation that could have an indirect effect on the nickel(II) environment. This could also mean that in the AlPO framework Ni(II) occupies somewhat different sites than Mn(II) and Co(II).

Acknowledgements. – Support by the Ministry of Science and Technology of the Republic of Slovenia, and International Büro Jülich (Germany) is acknowledged. M. Tisher from HASYLAB, Hamburg provided expert advice on beamline operation.

REFERENCES

1. E. M. Flanigen, B. M. Lok, R. L. Patton, and S. T. Willson, *New Developments in Zeolite Science Technology*, in: A. Murakami, A. Iikima, and J. W. Ward (Eds.), *Proceedings of the 7th International Zeolite Conference*, Kodansha, Tokyo, 1986, pp. 103–112.
2. N. Rajić, Dj. Stojaković, and V. Kaučič, *Zeolites* **11** (1991) 612–616.
3. N. Rajić, A. Ristić, and V. Kaučič, *Zeolites* **17** (1996) 304–309.

4. A. A. Verberckmoes, M. G. Uytterhoeven, and R. A. Schoonheydt, *Zeolites* **17** (1997) 180–189.
5. Ch. Lepetit and M. Che, *J. Phys. Chem*. **100** (1996) 3137–3143.
6. D. B. Akolekar and R. F. Howe, *J. Chem. Soc., Faraday Trans.* **93** (1997) 3263–3268.
7. U. Lohse, A. Bruckner, E. Schreier, R. Bertram, J. Janchen, and R. Fricke, *Microporous Materials* **1** (1996) 139–149.
8. A. M. Prakash, M. Hartmann, and L. Kevan, *J. Chem. Soc., Faraday Trans.* **93** (1997) 1233–1241.
9. L. Marchese, J. Chen, J. M. Thomas, S. Coluccia, and A. Zecchina, *J. Phys. Chem.* **98** (1994) 13350–13356.
10. L. Canesson, Y. Boudeville, and A. Tuel, *J. Am. Chem. Soc*. **119** (1997) 10754–10762.
11. H. Berndt, A. Martin, and Y. Zhang, *Microporous Materials* **6** (1996) 1–12.
12. T. I. Morrison, L. E. Iton, G. K. Shenoy, G. D. Stucky, S. L. Suib, and A. H. Reis, Jr., *J. Chem. Phys.* **73** (1980) 4705–4706.
13. T. I. Morrison, A. H. Reis, Jr., E. Gebert, L. E. Iton, G. D. Stucky, and S. L. Suib, *J. Chem. Phys.* **72** (1980) 6276–6282.
14. T. I. Morrison, L. E. Iton, G. K. Shenoy, G. D. Stucky, and S. L. Suib*, J. Chem. Phys.* **75** (1981) 4086–4089.
15. E. Dooryhee, C. R. A. Catlow, J. W. Couves, P. J. Maddox, J. M. Thomas, G. N. Greaves, A. T. Steel, and R. P. Townsend, *J. Phys. Chem*. **95** (1991) 4514–4521.
16. P. A. Barrett, G. Sankar, C. R. A. Catlow, and J. M. Thomas, *J. Phys. Chem*. **100** (1996) 8977–8985.
17. P. A. Barrett, G. Sankar, C. R. H. Jones, C. R. A. Catlow, and J. M. Thomas*, J. Phys. Chem. B* **101** (1997) 9555–9562.
18. C. Schott-Darie, H. Kessler, and E. Benazzi, in: T. Hattori and T. Yashima (Eds.), *Proceedings of the International Symposium on Zeolites Microporous Crystals (Nagoya, Japan, 1993)*, Elsevier, Amsterdam, 1994, pp. 3–10.
19. F. A. Cotton, G. Wilkinson, and P. L. Gaus, *Basic Inorganic Chemistry*, 3rd ed., John Wiley & Sons, New York, 1995, p. 540.
20. N. Rajić, A. Ristić, A. Tuel, and V. Kaučič, *Zeolites* **18** (1997) 115–118.
21. K. Seff, *Acc. Chem. Res.* **9** (1976) 121–128.
22. I. F. Chang and G. A. Sai-Halasz, *J. Electrochem. Soc*. **127** (1980) 2458–2464.
23. A. B. P. Lever, *Inorganic Electronic Spectroscopy*, 2rd ed., Elsevier, Amsterdam, 1984, p. 434.
24. W. W. Porterfield, *Inorganic Chemistry – A Unified Approach*, Academic Press, San Diego, 1993, p. 494.
25. A. B. P. Lever, *Inorganic Electronic Spectroscopy*, 2rd ed., Elsevier, Amsterdam, 1984, p. 533.
26. A. Bianconi, E. Fritsch, G. Calas, and J. Petiau, *Phys. Rev. B* **32** (1985) 4292–4295.
27. A. Bianconi, J. Garcia, and M. Benfatto, *Topics in Current Chemistry 145*, in: E. Mandelkow (Ed.), *Synchrotron Radiation in Chemistry and Biology I*, Springer Verlag, Berlin, 1988, pp. 29–68.
28. J. Wong, F. W. Lytle, R. P. Messmer, and D. H. Maylotte, *Phys. Rev. B* **30** (1984) 5596–5610.
29. A. Pantelouris, G. Küper, J. Hormes, C. Feldman, and M. Jansen, *J. Am. Chem. Soc*. **117** (1995) 11749–11753.

30. A. G. Sharpe, *Inorganic Chemistry*, 2rd ed., Longman, London, 1986, p. 590.
31. E. A. Stern, M. Newville, B. Ravel, Y. Yacoby, and D. Haskel, *Physica B* **208&209** (1995) 117–120.
32. J. Rehr, R. C. Albers, and S. I. Zabinsky, *Phys. Rev. Lett*. **69** (1992) 3397–3400.
33. A. Tuel, I. Arcon, N. Novak Tusar, A. Meden, and V. Kaučič, *Microporous Materials* **7** (1996) 271–284.
34. V. Kurshev, L. Kevan, D. Parillo, and R. Gorte, *Zeolite Science 1994: Recent Progress and Discussions*, in: H. G. Karge and J. Weitkamp (Eds.), *Stud. Surf. Sci. Catal*. **98** (1995) 79–80.
35. L. Canesson, I. Arcon, S. Caldarelli, and A. Tuel, *Microporous and Mesoporous Materials* **26** (1998) 117–131.
36. F. Shriver, P. W. Atkins, and C. H. Langford, *Inorganic Chemistry*, 2rd ed., Oxford University Press, Oxford, 1994, p. 246.

SAŽETAK

Istraživanje okruženja Mn, Co i Ni u formalno sintetiziranim te rehidratiziranim i kalciniranim aluminofosfatima topologije chabazita

Nevenka Rajić, Iztok Arčon, Venčeslav Kaučič i Alojz Kodre

Za istraživanje bliskog okruženja Mn, Co i Ni u materijalima opće formule MnAlPO, CoAlPO i NiAlPO s topologijom sličnoj chabazitu primijenjene su difuzno-refleksna spektroskopija (diffuse-reflectance spectroscopy, DRS) te metode apsorpcije rentgenskih zraka XANES (X-ray absorption near-edge structure) i EXAFS (extended X-ray absorption fine structure). U sva tri nastala proizvoda ustanovljena je zamjena atoma aluminija atomom prijelaznog metala u tetraedarskoj šupljini koju u strukturi zaposjeda aluminij. Kalcinacija i rehidratacija takvih formalno sintetiziranih materijala prouzročila je promjenu oksidacijskog broja i koordinacijske geometrije Mn i Co dok su oksidacijski i koordinacijski broj Ni ostali netaknuti.